Proceedings of the ASME 2011 International Mechanical Engineering Congress & Exposition
IMECE 2011
November 11-17, 2011, Denver, Colorado, USA

IMECE2011/62608

A CHAOTIC BLUE SKY CATASTROPHE OF BUTTERFLY VALVES DRIVEN BY SOLENOID ACTUATORS

Peiman Naseradinmousavi
Center for Nonlinear Dynamics and Control (CENDAC)
Department of Mechanical Engineering
Villanova University
Villanova, Pennsylvania 19085
Email: pnaser01@villanova.edu

C. Nataraj
Professor and Chair
Department of Mechanical Engineering
Villanova University
Villanova, Pennsylvania 19085
Email: nataraj@villanova.edu

ABSTRACT

Chilled water systems used in the industry and on board ships are critical for safe and reliable operation. It is hence important to understand the fundamental physics of these systems. This paper focuses in particular on a critical part of the automation system, namely, actuators and valves that are used in so-called "smart valve" systems. The system is strongly nonlinear, and necessitates a nonlinear dynamic analysis to be able to predict all critical phenomena that affect effective operation and efficient design. The derived mathematical model includes electromagnetics, fluid mechanics, and mechanical dynamics. Nondimensionalization has been carried out in order to reduce the large number of parameters to a few critical independent sets to help carry out a broad parametric analysis. The system stability analysis is then carried out by the aid of the tools from nonlinear dynamic analysis. This reveals that the system is unstable in a certain region of the parameter space. The system is also shown to exhibit crisis and chaotic responses; this is characterized using Lyapunov exponents and power spectra. Knowledge and avoidance of these dangerous regimes is necessary for successful and safe operation.

INTRODUCTION

Modeling and designing accurate shipboard machinery systems has received much attention as one of the important challenges that needs to be overcome for supporting the next generation Naval machinery automation requirements [1]. Typical automation systems used in the US Navy consist of actuators, sensors, controllers, valves, piping, electrical cabling and communication wiring. Many types of actuator-valve systems are in use [2, 3].

In general, these systems are nonlinear and exhibit nonlinear phenomena such as multiple steady solutions, bifurcations, multi-frequency responses, and chaotic dynamics. All of these phenomena have been observed in practice but cannot be explained even qualitatively by traditional linear theories used in engineering practice.

This paper focuses in particular on a critical part of the automation system, namely, actuator-valve systems that form an important part of what are termed "smart valve" systems. All of these systems are nonlinear and need to be analyzed as such. Nonlinear dynamic analysis of such an interdisciplinary system is not trivial, but needs to be investigated in order to predict possible critical phenomena including chaos and its routes.

Specific work related to the system considered here is somewhat difficult to find; however, there has indeed been much research in related areas and is discussed here. Important nonlinear phenomena in electromechanical systems such as chaos have received considerable attention by researchers. Belato *et al.* [4] analyzed chaotic vibrations of an electromechanical system which includes a nonlinear dynamic system consisting of a simple pendulum whose support point is vibrated along a horizontal guide by a two bar linkage driven by a DC motor with limited power.

Nonlinear dynamic analysis of a micro electromechanical system (MEMS) has been carried out by Xie *et al.* [5] based on an invariant manifold method proposed by Boivin *et al.* [6]. Ge and Lin [7] have studied dynamical analysis of electromechanical gyrostat system subjected to external disturbance.

Chaotic responses are distinguishable by sensitivity to initial conditions which are examined in this paper. Power spectra and Lyapunov exponents are also helpful to identify chaotic system responses since they exhibit a broadband power spectrum, and one or more positive Lyapunov exponents must be observed [8].

The first part of the paper deals with a high-fidelity mathematical model, and the second part deals with nonlinear dynamic analysis of the system. This paper follows on the previous work carried out by the authors [9].

MATHEMATICAL MODELING

The system consists of a solenoid actuator energized by an electric voltage (DC or AC) which moves a plunger. The plunger is connected to a butterfly valve through a rack and pinion arrangement as shown in Fig. 1. The magnetic flux generates the needed electromagnetic force to move the plunger and subsequently results in the rotation of the butterfly valve by the coupled rack and pinion mechanism.

An ideal pressure angle is assumed for the rack and pinion mechanism with an assumption of no backlash of the gears. The valve controls the flow in a pipe and is hence subject to hydrodynamic forces.

Electromagnetics

The magnetic force is calculated using the reluctance method [9] as follows.

$$F_m = \frac{R_2 N^2 i^2}{2(R_1 + R_2(g_0 - x))^2} \tag{1}$$

where, g_0 indicates the maximum stroke of the plunger, x is the displacement of solenoid plunger, and, R_1 and R_2 are the reluctances of the magnetic flux paths. A simple circuit model leads to the following mathematical model.

$$\frac{di}{dt} = \frac{(V - Ri)(R_1 + R_2(g_0 - x))}{N^2} - \frac{R_2 i\dot{x}}{(R_1 + R_2(g_0 - x))} \tag{2}$$

Fluid Mechanics

Analysis must be done on the hydrodynamic (T_h), bearing (T_b), and seating (T_s) torques as they are highly nonlinear functions affecting the valve rotation angle. The torque terms are

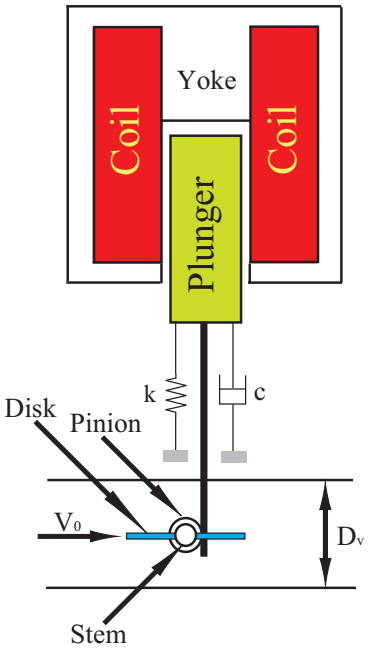

FIGURE 1. SCHEMATIC MODEL OF THE SYSTEM

given as follows [10–14].

$$T_h = \frac{8\rho T_c D_v^3 V_0^2}{3\pi} \underbrace{\frac{4}{[C_{cc}(1-\sin\alpha)]^2}}_{\left(\frac{V_J}{V_0}\right)^2} \tag{3}$$

$$T_b = -\frac{\pi}{8}\mu D_s D_v^2 \Delta P \text{sign}(\dot{\alpha}) \tag{4}$$

$$T_s = C_s D_v^2 \tag{5}$$

where, ρ is the fluid density; α is the valve rotation angle; T_c indicates the torque coefficient which can be calculated by a table look up for various values of α, based on Computational Fluid Dynamics calculations, as shown in Fig. 2; D_v is the pipe diameter; V_0 indicates the inlet velocity of flow; V_J is the jet velocity; C_{cc} is the sum of upper and lower contraction coefficients and is shown in Fig. 3; D_s is the stem diameter; μ indicates the friction coefficient of the bearing area; C_s is the coefficient of the seating area; and,

$$\Delta P = \frac{1}{2}\rho V_0^2 \left(\frac{V_J}{V_0} - 1\right)^2 \tag{6}$$

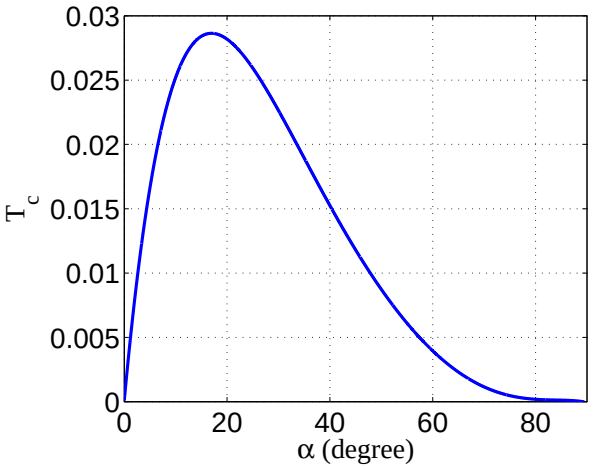

FIGURE 2. HYDRODYNAMIC TORQUE COEFFICIENT VS. α

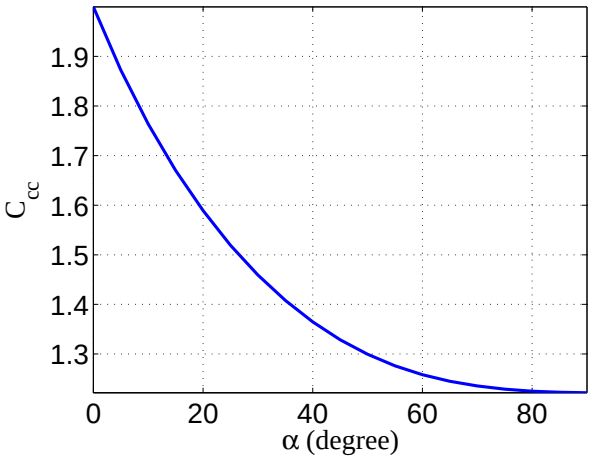

FIGURE 3. C_{cc} VS. α

indicates the pressure drop across the valve.

Dynamics

The dynamical equations of the plunger and butterfly valve can be written as follows (Fig. 4).

$$m\ddot{x} + c\dot{x} + kx = F_m - F_c \tag{7}$$

$$J\ddot{\alpha} + b\dot{\alpha} = rF_c + T_h - T_b\text{sign}(\dot{\alpha}) - T_s \tag{8}$$

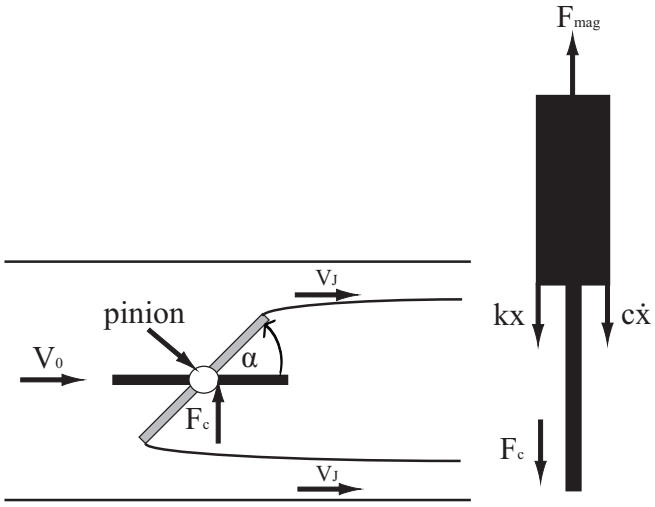

FIGURE 4. FREE BODY DIAGRAMS OF THE SOLENOID ACTUATOR AND THE BUTTERFLY VALVE

In addition, we have the kinematic constraint between the rack and the pinion,

$$x = r\alpha. \tag{9}$$

Combining Eqs. 1, 3, 4, 5, 7, and 8, one has,

$$\begin{aligned}&\left(mr^2+J\right)\ddot{\alpha} + \left(cr^2+b\right)\dot{\alpha} + kr^2\alpha = \\ &\frac{rR_2N^2i^2}{2(R_1+R_2(g_0-r\alpha))^2} + \frac{32\rho T_c D_v^3 V_0^2}{3\pi[C_{cc}(1-\sin(\alpha))]^2} \\ &- \frac{\pi}{16}\mu\rho D_s D_v^2 V_0^2 \text{sign}(\dot{\alpha})\left(\frac{2}{C_{cc}(1-\sin(\alpha))}-1\right)^2 \\ &- C_s D_v^2\end{aligned} \tag{10}$$

Note that C_{cc} and T_c are dependent on α. Eqs. (2) and (10) constitute the third order dynamic model for the system.

NONDIMENSIONALIZATION

In order to reduce the number of parameters, and to perform a systematic analysis, the nonlinear dynamic equations need to be nondimensionalized. We define the state vector as $x = [\alpha, \dot{\alpha}, i]^T$, and derive the nondimensionalized state-space equations as follows.

$$\dot{x}_1 = x_2 \tag{11}$$

$$\begin{aligned}\dot{x}_2 = &-x_1 - 2\zeta x_2 + \frac{\vartheta x_3^2}{\left(\Delta_1 + \Delta_2(\gamma - x_1)\right)^2} + (x_1(\beta_1 e^{ax_1} + \beta_2)) \\ &- \text{sign}(x_2)(\kappa_1 x_1^2 e^{\kappa_2 x_1} + \kappa_3 e^{\kappa_4 x_1}) - \frac{C_s D_v^2}{\omega_{n0}^2(J+mr^2)}\end{aligned} \tag{12}$$

$$\dot{x}_3 = \frac{(v-x_3)(\Delta_1+\Delta_2(\gamma-x_1))}{N^2} - \frac{\Delta_2 x_2 x_3}{(\Delta_1+\Delta_2(\gamma-x_1))} \tag{13}$$

Here,

$$\omega_{n0} = \sqrt{\frac{kr^2}{J+mr^2}}; \gamma = \frac{g_0}{r}; \Delta_1 = \frac{RR_1}{\omega_{n0}}; \Delta_2 = \frac{RR_2 r}{\omega_{n0}}$$

$$\zeta = \frac{(b+cr^2)}{2\omega_{n0}(J+mr^2)}; \vartheta = \frac{rR_2N^2i_0^2R^2}{2\omega_{n0}^4(J+mr^2)}$$

The values of β_1, β_2, a, κ_1, κ_2, κ_3 and κ_4 are calculated based on fitting the torques to the following functions with least square error.

$$T_{\text{hnd}} = \beta_1 \alpha e^{a\alpha} + \beta_2 \alpha \tag{14}$$

$$T_{\text{bnd}} = \kappa_1 \alpha^2 e^{\kappa_2 \alpha} + \kappa_3 e^{\kappa_4 \alpha} \tag{15}$$

NONLINEAR ANALYSIS

The model has twelve nondimensional parameters; the analysis presented in this paper assumes specific values for ten of them as shown in Table 1; these values are based on realistic parameter values for an industrial system. Two parameters, ϑ and ζ are considered to vary over a range of values.

The sign function is replaced by a differentiable function to make the linearization process easier. A smooth approximation of the sign function is,

$$\text{sign}(x_2) \approx \tanh(Kx_2) \tag{16}$$

where, k can be tuned to get a good approximation; we used $k = 1$ in this analysis.

The Jacobian matrix for the system can be calculated as follows.

$$J = \begin{bmatrix} 0 & 1 & 0 \\ A_0 & A_1 & \frac{2\vartheta x_{30}}{(\Delta_1+\Delta_2(\gamma-x_{10}))^2} \\ B_0 & -\frac{\Delta_2 x_{30}}{(\Delta_1+\Delta_2(\gamma-x_{10}))} & C_0 \end{bmatrix} \tag{17}$$

where,

$$A_0 = \frac{2\vartheta x_{30}^2 \Delta_2}{(\Delta_1+\Delta_2(\gamma-x_{10}))^3} + \beta_1 e^{ax_{10}}(1+ax_{10})$$

TABLE 1. Nondimensional parameters

β_1	7×10^{-4}	a	5.2764
β_2	0.44	γ	1.8
κ_1	1×10^{-7}	κ_2	13.62
κ_3	-0.5	ζ	varies
κ_4	-13	ϑ	varies
Δ_1	536		
Δ_2	1×10^4		

$$+ \beta_2 - 1 \tag{18}$$

$$A_1 = -2\zeta - K(1-\tanh^2 Kx_{20})(\kappa_1 x_{10}^2 e^{\kappa_2 x_{10}} + \kappa_3 e^{\kappa_4 x_{10}}) \tag{19}$$

$$B_0 = -\frac{\Delta_2(v-x_{30})}{N^2} - \frac{\Delta_2^2 x_{20} x_{30}}{(\Delta_1+\Delta_2(\gamma-x_{10}))^2} \tag{20}$$

$$C_0 = -\frac{\Delta_1+\Delta_2(\gamma-x_{10})}{N^2} - \frac{\Delta_2 x_{20}}{\Delta_1+\Delta_2(\gamma-x_{10})} \tag{21}$$

and $[x_{10}, x_{20}, x_{30}]$ is an equilibrium point of the system.

For the linearized system, the characteristic equation becomes

$$s^3 + \left(2\zeta + \frac{\Delta_1+\Delta_2(\gamma-x_{10})}{N^2} + K\left(\kappa_1 x_{10}^2 e^{\kappa_2 x_{10}} + \kappa_3 e^{\kappa_4 x_{10}}\right)\right)s^2 + \left(\left(2\zeta + K(\kappa_1 x_{10}^2 e^{\kappa_2 x_{10}} + \kappa_3 e^{\kappa_4 x_{10}})\right) \times \left(\frac{\Delta_1+\Delta_2(\gamma-x_{10})}{N^2}\right) + 1 - (\beta_1 e^{ax_{10}}(1+ax_{10}) + \beta_2)\right)s + A_0 C_0 = 0 \tag{22}$$

Using Routh-Hurwitz criteria, one is able to judge the system's linear stability behavior. The asymptotical stability requirements of the system can then be determined as follows.

$$\frac{2\vartheta x_{30}^2 \Delta_2}{(\Delta_1+\Delta_2(\gamma-x_{10}))^3} + \beta_1 e^{ax_{10}}(1+ax_{10}) + \beta_2 < 1 \tag{23}$$

$$\frac{4\zeta^2(\Delta_1+(\gamma-x_{10})\Delta_2)}{N^2} + \frac{2\zeta(\Delta_1+(\gamma-x_{10})\Delta_2)^2}{N^4} + \frac{2\vartheta x_{30}^2 \Delta_2}{N^2(\Delta_1+(\gamma-x_{10})\Delta_2)^2} + 4\zeta K(\kappa_1 x_{10}^2 e^{\kappa_2 x_{10}} \kappa_3 e^{\kappa_4 x_{10}}) \times \frac{(\Delta_1+(\gamma-x_{10})\Delta_2)}{N^2} + 2\zeta + K(\kappa_1 x_{10}^2 e^{\kappa_2 x_{10}} + \kappa_3 e^{\kappa_4 x_{10}}) \times \frac{(\Delta_1+(\gamma-x_{10})\Delta_2)^2}{N^4} + K^2(\kappa_1 x_{10}^2 e^{\kappa_2 x_{10}} + \kappa_3 e^{\kappa_4 x_{10}})^2$$

$$\times \frac{(\Delta_1+(\gamma-x_{10})\Delta_2)}{N^2}+K(\kappa_1 x_{10}^2 e^{\kappa_2 x_{10}}+\kappa_3 e^{\kappa_4 x_{10}})$$
$$> 2\zeta(\beta_1 e^{ax_{10}}(1+ax_{10})+\beta_2)+K(\kappa_1 x_{10}^2 e^{\kappa_2 x_{10}}+\kappa_3 e^{\kappa_4 x_{10}})$$
$$\times (\beta_1 e^{ax_{10}}(1+ax_{10})+\beta_2) \quad (24)$$

It can be shown from Eq. 23 that the system reveals an unstable response unless k is large enough which reduce the value of β_2.

Eq. 24 yields a comprehensive relationship to examine the system stability by varying the critical parameters such as ζ (equal viscous damping) and ϑ (magnetic force parameter).

Fig. 5 illustrates the range of ζ vs. ϑ obtained from the calculated stability criteria where the stable and unstable regions can be distinguished. A confirmation of the stability map is shown in Fig. 6 revealing the stable behavior of the system for $\zeta = 0.5$ and $\vartheta = 4.8\times10^5$; the system's unstable behavior can be observed from Fig. 7 where the response diverges to infinity.

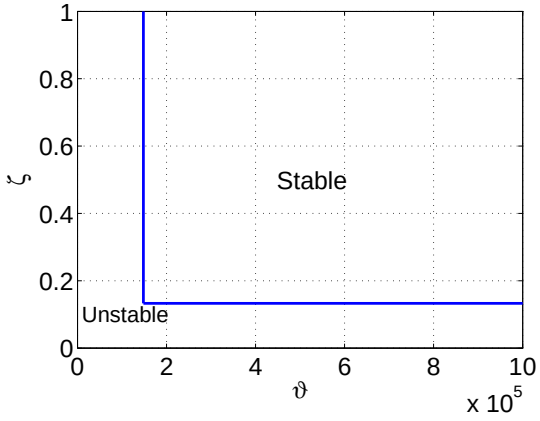

FIGURE 5. STABILITY MAP IN THE (ζ AND ϑ) PARAMETER PLANE

Next, we investigate the system responses for variations of ζ and ϑ. Shown in Fig. 8 indicates a trapped chaotic motion between two stable regions using a marginal value of ζ.

The Lyapunov exponents of such a motion shown in Fig. 9 confirm the observed chaotic motion; one positive Lyapunov exponent is distinguishable. Note that the positive value is not big enough to yield a chaotic motion forever and its effects finally will be mitigated by the largest negative value of Lyapunov exponents ($|\lambda_3| \approx 10|\lambda_1|$).

Shown in Fig. 10 is the power spectrum indicating noisy characteristic typical of chaotic responses for a certain range of frequencies.

Zeeman [15] defines a catastrophe to be any discontinuous bifurcation. Abraham and Stewart [16] have been more specific

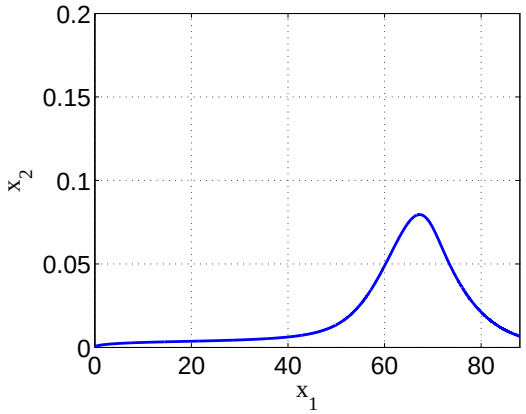

FIGURE 6. THE SYSTEM RESPONSE FOR $\zeta = 0.5$ AND $\vartheta = 4.8\times10^5$

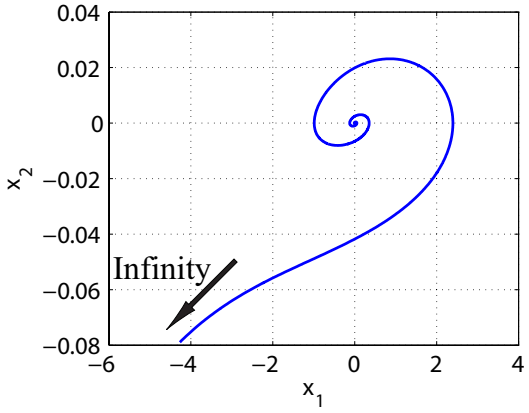

FIGURE 7. THE SYSTEM RESPONSE FOR $\zeta = 0.05$ AND $\vartheta = 1\times10^3$

and define blue sky catastrophe - a bifurcation in which an entire attractor disappears abruptly from the phase portrait as a control parameter α passes through its critical value α_c; when such a bifurcation occurs, the dynamical system will make a finite jump to a remote attractor, or diverge to infinity [17].

A small change in the critical value of $\zeta(0.133)$ yields such a phenomenon (crisis) shown in Fig. 11 where a chaotic attractor abruptly disappears for $\zeta = 0.1329$ and diverges to infinity. It can also be validated from Fig. 12 where its Lyapunov exponents, having at least one positive value for a chaotic motion, suddenly disappear.

CONCLUSION

This paper developed accurate nonlinear dynamic models of butterfly valves operated by solenoid actuators. Many tools from

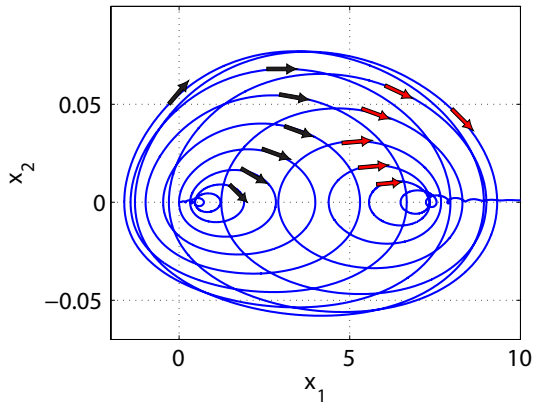

FIGURE 8. PHASE PORTRAIT FOR $\zeta = 0.133$ AND $\vartheta = 1.48 \times 10^5$

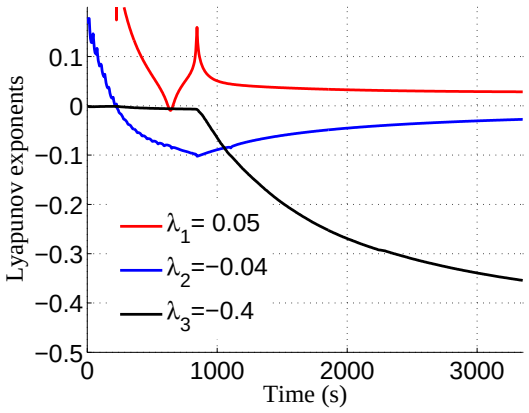

FIGURE 9. LYAPUNOV EXPONENTS FOR $\zeta = 0.133$ AND$\vartheta = 1.48 \times 10^5$

nonlinear dynamic analysis were then utilized to investigate the system stability and distinguish between the responses for a set of parameters.

The variations of two critical parameters, ζ and ϑ, were then studied to establish stability regimes and to investigate harmful nonlinear phenomena such as chaos and crisis.

Lyapunov exponents were calculated displaying one positive value and the power spectrum showed a noisy nature confirming the chaotic nature of the response for a certain period of time. Also observed for some parametric value was a blue sky catastrophe phenomenon, which is distinguishable by the disappeared chaotic attractor and its divergence to infinity when the control parameter passes through its critical value.

Determining the critical range of these parameters is an important step that needs to be taken for safe operation of the system. Current work is focusing on experimental validation of these theoretical results.

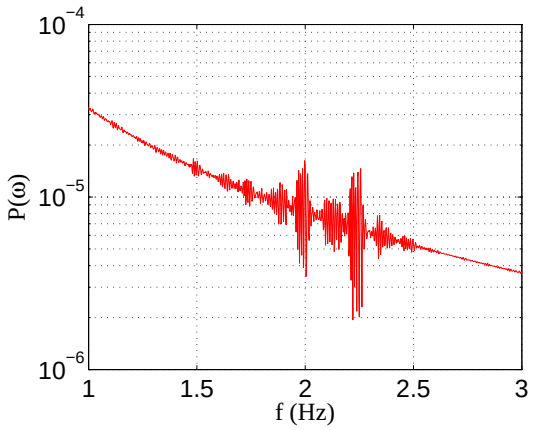

FIGURE 10. POWER SPECTRUM FOR $\zeta = 0.133$ AND $\vartheta = 1.48 \times 10^5$

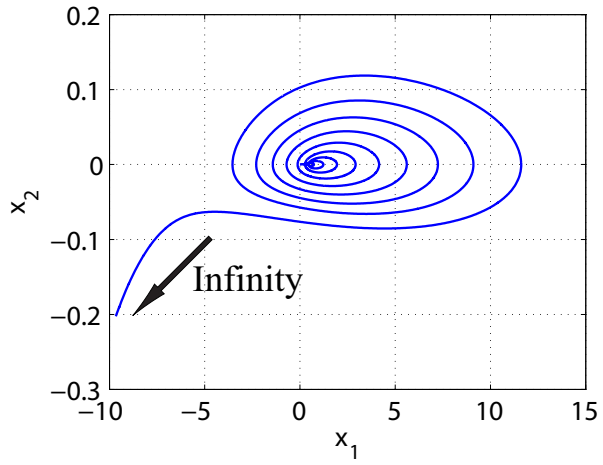

FIGURE 11. PHASE PORTRAIT FOR $\zeta = 0.1329$ AND $\vartheta = 1.48 \times 10^5$

ACKNOWLEDGMENT

This work was supported by Office of Naval Research Grant (N00014/08/1/0435). The authors are grateful to ONR, and Mr. Anthony Seman III in particular, for the financial support that made this research possible. Thanks are also due to Dr. Stephen Mastro and Mr. Frank Ferrese of Naval Surface Warfare Center (Philadelphia) for valuable help and guidance.

REFERENCES

[1] Fairmount Automation, 2005. “DDG-51 Class chilled water automation systems (CWAS) land-

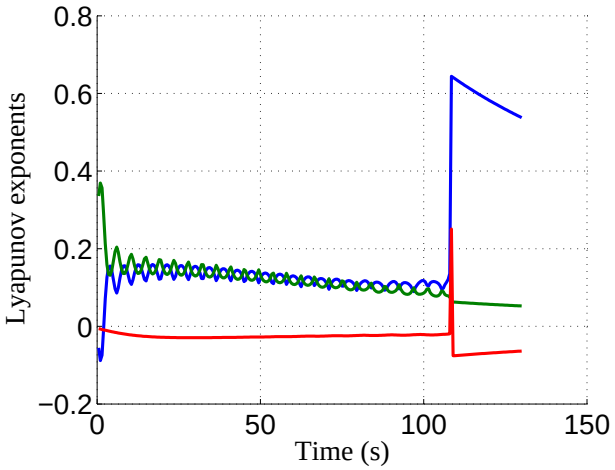

FIGURE 12. LYAPUNOV EXPONENTS FOR $\zeta = 0.1329$ AND $\vartheta = 1.48 \times 10^5$

based performance test (LBPT) facility control and monitoring system (CMS)". See also URL http://www.fairmountauomation.com.

[2] Hughes, R., Balestrini, S., Kelly, K., Weston, N., Mavris, D., 2006. "Modeling of an Integrated Reconfigurable Intelligent System (IRIS) for Ship Design". *ASNE Ships and Ship Systems Symposium*.

[3] Lequesne, B., Henry, R., Kamal, M., 1988. Magnavalve: A New Solenoid Configuration Based on a Spring-Mass Oscillatory System for Engine Valve Actuation. GM Research Report, E3-89.

[4] Belato, D., Weberb, H. I., Balthazarc, J. M., Mook, D. T., 2001. "Chaotic Vibrations of a Nonideal Electro-Mechanical System". *International Journal of Solids and Structures*, **38**(10-13), pp. 1699-1706.

[5] Xie, W. C., Lee, H. P., Lim, S. P., 2004. "Nonlinear Dynamic Analysis of MEMS Swithes by Nonlinear Modal Analysis". *Journal of Nonlinear Dynamics*, **31**, pp. 243-256.

[6] Boivin, N., Pierre C., Shew, S. W., 1885. "Nonlinear Normal Modes, Invariance, and Modal Dynamics Approximations of Nonlinear Systems". *Journal of Nonlinear Dynamics*, **8**, pp.315-346.

[7] Ge, Z. M., Lin, T. N., 2003. "Chaos, Chaos Control and Synchronization of Electro-Mechanical Gyrostat System". *Journal of Sound and Vibration*, **259**(3), pp. 585-603.

[8] Nayfeh, A. H, Balachandran, B., 1995. *Applied nonlinear dynamics: analytical, computational, and experimental methods*, Wiley-VCH Verlag GmbH, Weinheim, Germany.

[9] Naseradinmousavi, P., Nataraj, C., 2011. "Nonlinear Mathematical Modeling of Butterfly Valves Driven by Solenoid Actuators". *Jouranl of Applied Mathematical Modelling*, **35**(5), pp. 2324-2335.

[10] Park, J. Y., Chung M. K., 2006. "Study on Hydrodynamic Torque of a Butterfly Valve". *Journal of Fluids Engineering*, **128**, pp. 190-195.

[11] Sarpkaya, T., 1959. "Oblique Impact of a Bounded Stream on a Plane Lamina". *Journal of the Franklin Institue*, **267**(3), pp. 229-242.

[12] Sarpkaya, T., 1961. "Torque and Cavitation Characteristics of Butterfly Valves". *ASME Journal of Applied Mechanics*, **28**(4), pp. 511-518.

[13] Ogawa, K., Takeyoshi, T., 1995. "Hydrodynamic Characteristics of a Butterfly Valve - Prediction of Torque Characteristics". *ISA Transactions*, **34**(4), pp. 327-333.

[14] Leutwyler, Z., Dalton C., 2008. "Resultant Force, and Aerodynamic Torque on a Symmetric Disk Butterfly Valve in a Compressible Flow". *Journal of Pressure Vessel Technology*, **130**, May.

[15] Zeeman, E. C., 1982. "Bifurcation and Catastrophe Theory", *Papers in Algebra, Analysis, and Statistics, R. Lidl, ed.*.

[16] Abraham, R. H., Stewart., H. B., 1986. " A Chaotic Blue Sky Catastrophe in Forced Relaxation Oscillators", *Physics 21D*, pp. 394-400.

[17] Stewart, H. B., Thompson, J. M. T., 1986. "Towards a Classification of Generic Bifurcations of Dissipative Dynamical Systems", *Dyn. Stab. Syst. 1*.